JOURNAL OF BACTERIOLOGY, Mar. 1987, p. 1071–1079
0021-9193/87/0301071-09$02.00/0

Vol. 169, No. 3

An Unusual Genetic Link between Vitamin B_6 Biosynthesis and tRNA Pseudouridine Modification in *Escherichia coli* K-12

PEGGY J. ARPS AND MALCOLM E. WINKLER*

Department of Molecular Biology, Northwestern University Medical School, Chicago, Illinois 60611

Received 29 August 1986/Accepted 2 December 1986

We characterized several unusual phenotypes caused by stable insertion mutations in a gene that is located upstream in the same operon from *hisT*, which encodes the tRNA modification enzyme pseudouridine synthase I. Mutants containing kanamycin resistance (Km^r) cassettes in this upstream gene, which we temporarily designated *usg-2*, failed to grow on minimal plus glucose medium at 37 and 42°C. However, *usg-2*::Km^r mutants did form oddly translucent, mucoid colonies at 30°C or below. Microscopic examination revealed that cells from these translucent colonies were spherical and seemed to divide equatorially. Addition of D-alanine restored the shape of the mutant cells to rods and allowed the mutants to grow slowly at 37°C and above. By contrast, addition of the common L-amino acids prevented growth of the *usg-2*::Km^r mutants, even at 30°C. Furthermore, prolonged incubation of *usg-2*::Km^r mutants at 37 and 42°C led to the appearance of several classes of temperature-resistant pseudorevertants. Other compounds also supported growth of *usg-2*::Km^r mutants at 37 and 42°C, including glycolaldehyde and the B_6 vitamers pyridoxine and pyridoxal. This observation suggested that *usg-2* was *pdxB*, which had been mapped near *hisT*. Complementation experiments confirmed that *usg-2* is indeed *pdxB*, and inspection of the pyridoxine biosynthetic pathway suggests explanations for the unusual phenotypes of *pdxB*::Km^r mutants. Finally, Southern hybridization experiments showed that *pdxB* and *hisT* are closely associated in several enterobacterial species. We consider reasons for grouping *pdxB* and *hisT* together in the same complex operon and speculate that these two genes play roles in the global regulation of amino acid metabolism.

Knowledge of the structure and regulation of operons that encode enzymes involved in single metabolic pathways such as *ara*, *gal*, *his*, *lac*, and *trp* has provided many of the fundamental concepts and tools of molecular genetics (5, 33, 38, 41). However, enterobacteria also contain a class of operons about which much less is known. These multifunctional operons are distinguished from single-pathway operons by their composition and complex regulation. For example, operons that encode ribosomal proteins include genes for proteins involved in translation such as EF-Ts, EF-Tu, EF-G, and PheRS and genes for proteins involved in RNA metabolism such as the subunits of RNA polymerase, tRNA (m^1G) methyltransferase, polynucleotide phosphorylase, DNA primase, and RNase P (see references in reference 9). The reason for grouping ribosomal protein genes in the same operon with these other genes presently is not well understood, although it is assumed that this type of arrangement allows coordinate regulation of the different classes of genes under some culture conditions (9, 34). This notion is supported by the finding that the gene arrangements of certain multifunctional operons appear to be evolutionarily conserved in different bacterial species (13, 47). Of the ribosomal protein operons, the regulatory signals of the *rpsU-dnaG-rpoD* macromolecular synthesis (sigma) operon are the best characterized. The array of multiple primary promoters, a *lexA* operator, an antitermination site, a nonregulated attenuator, internal promoters including one sensitive to heat shock, and an RNA processing site underscores the complex, multivalent regulation of the macromolecular synthesis operon (34). Other multifunctional operons also appear to be subject to complex modes of regulation (9).

Recently, we reported that *hisT*, which encodes the tRNA modification enzyme pseudouridine synthase I, is part of a complex, multifunctional operon in *Escherichia coli* K-12 (2; 36; see accompanying paper [3]). Using a combination of approaches, we have shown that the *hisT* operon contains at least four genes whose functions appear to be unrelated (Fig. 1) (see reference 3). If we are to understand why *hisT* is part of a complex operon, we must identify these other genes. To this end, we characterized the physiology of bacteria containing kanamycin resistance (Km^r) cassettes at various chromosomal sites near *hisT*. Mutants containing insertions in the gene designated *usg-2* were particularly amenable to study, because *usg-2*::Km^r mutants, unlike insertion mutants of *usg-1*, *hisT*, or *dsg-1*, have a set of unusual auxotrophic phenotypes (2, 3; see below). In fact, we used these phenotypes as part of the evidence for the existence of *usg-2* as a gene upstream from *hisT* in the same operon (2, 3). In addition, we used Km^r cassettes to locate genetic signals near the end of the coding region for the 42,000-dalton *usg-2* polypeptide (3).

In this paper, we describe the unusual physiological characteristics of *usg-2*::Km^r mutants. These properties led to the identification of *usg-2* as *pdxB*, which mediates the biosynthesis of the pyridine ring of the B_6 vitamer pyridoxine. Pyridoxine in turn is a direct precursor of the essential coenzyme pyridoxal phosphate. Thus, the results presented here establish a novel genetic link between tRNA pseudouridine modification and vitamin B_6 biosynthesis. The implications of this finding to pyridoxal phosphate biosynthesis and control of the *pdx* regulon are also considered.

MATERIALS AND METHODS

Materials. Restriction endonucleases and T4 DNA ligase used in cloning were purchased from New England BioLabs, Inc. (Beverly, Mass.). DNA polymerase I large fragment used to fill in sites and DNA polymerase I used in nick

* Corresponding author.

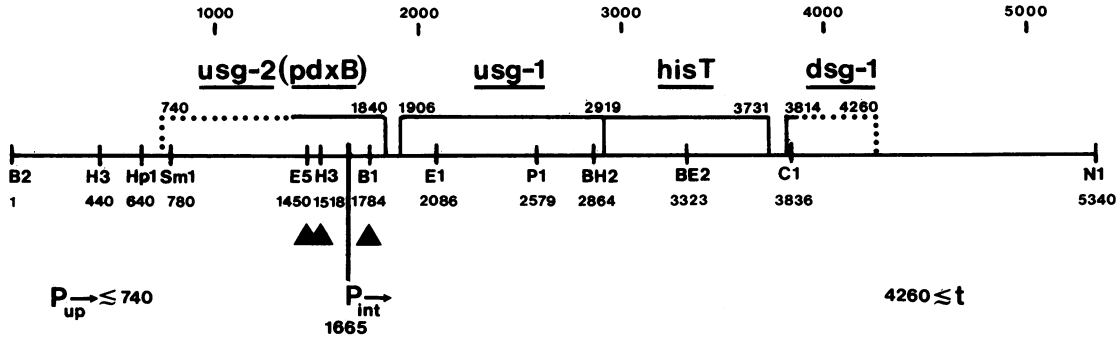

FIG. 1. Structure of the *hisT* operon. The boxes and numbers above the boxes show the coding regions of genes in the operon, where solid and dotted lines indicate exact and approximate boundaries (see accompanying paper [3]). The location of the internal promoter (P_{int}) and the approximate locations of at least one other promoter (P_{up}) and the terminator at the end of the operon (t) are shown. The positions of Km^r cassette insertion mutations used in this study are marked with solid triangles (▲) (Table 1). For clarity, *usg-2* is also designated as *pdxB* as shown in this paper. Abbreviations: B1, *Bgl*I; B2, *Bgl*II; BE2, *Bst*EII; BH2, *Bss*HII; C1, *Cla*I; E1, *Eco*RI; E5, *Eco*RV; H3, *Hin*dIII; Hp1, *Hpa*I; N1, *Nru*I; P1, *Pst*I; Sm1, *Sma*I.

translation reactions were purchased from Boehringer Mannheim Biochemicals (Indianapolis, Ind.). Antibiotics and biochemicals were from Sigma Chemical Co. (St. Louis, Mo.) and P-L Biochemicals, Inc. (Milwaukee, Wis.). Components of culture media were from Difco Laboratories (Detroit, Mich.). Formvar carbon-coated copper grids used in electron microscopy were purchased from Ernest F. Fullam, Inc. [α-^{32}P]dCTP (~3,000 Ci/mmol) used in nick translation reactions was purchased from Amersham Corp. (Arlington Heights, Ill.).

Bacterial strains, plasmids, media, and growth conditions. The bacterial strains and plasmids used in this study are listed in Table 1. Strains nearly isogenic to NU426 or CGSC 4805 were constructed by generalized transduction with P1 *kc* bacteriophage as described previously (3, 37). The kanamycin resistance (Km^r) cassette isolated from plasmid pMB2190 was cloned into plasmids and crossed into the bacterial chromosome as described in the accompanying paper (3) and in reference 54. DNA manipulations and cloning were performed by well-established procedures described previously (2, 3, 14, 35, 36).

Bacteria were cultured in LB medium supplemented with 30 μg of L-cysteine per ml (LB + Cys) and in Vogel-Bonner minimal (E) medium containing 0.4% (wt/vol) glucose (14). The concentrations of additional supplements are noted in the figures and tables. When required, ampicillin or kanamycin was added at a final concentration of 50 μg/ml. Other details about culture conditions are given in the figures and tables.

Southern hybridizations. Genomic DNA was isolated from the bacterial species indicated in Fig. 3 by the method of Driver and Lawther (22). Approximately 3 μg of each purified genomic DNA was digested with restriction endonucleases, resolved on a 0.8% agarose gel, denatured, and transferred to nitrocellulose filters as described previously (22, 35, 45). Restriction fragments containing segments of the coding regions of *pdxB*, *usg-1*, or *hisT* were isolated from plasmid pNU117, pNU118, or pNU119, respectively (Table 1). The separately cloned and isolated fragments were labeled with ^{32}P by nick translation as described previously (35) except that labeled DNA was precipitated with spermine to remove unincorporated [α-^{32}P]dCTP (27).

Moderately high stringency hybridizations of ^{32}P-labeled DNA probes to genomic DNA blotted onto nitrocellulose filters (10.5 by 13 cm) were completed as follows. A baked filter which was stored under vacuum at room temperature was wetted with water and sealed into a bag. A 5.0-ml portion of 50% formamide–6× SSC (1× SSC is 0.15 M NaCl plus 0.015 M sodium citrate, pH 7.0)–5× Denhardt mixture (1× Denhardt mixture is 0.02% [wt/vol] each of Ficoll, polyvinylpyrrolidone, and bovine serum albumin)–100 μg of sonicated salmon sperm DNA per ml–0.2% (wt/vol) sodium dodecyl sulfate (SDS) was heated for 10 min at 96°C, chilled quickly, and injected into the bag containing the filter. The bag was shaken gently for 3 h at 42°C. The prehybridization solution was then drained from the bag and discarded. A 5.0-ml portion of the same solution containing about 6×10^6 cpm (Cerenkov) of ^{32}P-labeled DNA probe was heated, chilled, and added to the bag. Hybridization was allowed to proceed for about 18 h at 42°C. The filters were removed from the bag, dipped into 2× SSC–0.2% (wt/vol) SDS to remove excess counts, washed at least four times for 30 min each in 250 ml of 2× SSC–0.2% (wt/vol) SDS at 42°C, dried on filter paper at room temperature, covered in plastic wrap, and autoradiographed in the presence of an intensifying screen at −20°C. Low stringency hybridization reactions were completed in two ways. In the first variation, the filters were treated as described above except that prehybridization (3 h), hybridization (36 h), and washes were all completed at room temperature. In the second variation, the prehybridization (3 h) and hybridization (36 h) solutions contained 25% formamide, 4× SSC, 5× Denhardt mixture, 100 μg of sonicated salmon sperm DNA per ml, and 0.2% SDS at 37°C, and the wash solution contained 5× SSC and 0.2% SDS at 55°C.

Microscopy. For light microscopy, a small portion of a bacterial colony was scraped from a plate that had incubated for 1 to 3 days and was either smeared directly onto a glass slide or suspended in a drop of minimal (E) medium on a slide. Bacterial cells were viewed at magnifications ranging from ×800 to ×2,000 with phase-contrast and oil immersion optics. For electron microscopy, bacterial cells were added to specimen grids, fixed with paraformaldehyde-glutaraldehyde, and stained with uranyl acetate as described by Hultgren et al. (30). Bacterial cells were viewed at a magnification of ×24,900.

RESULTS

Physiology and growth characteristics of *usg-2*::Km^r cassette mutants. To study the organization and expression of

TABLE 1. Bacterial strains and plasmids

Strain or plasmid	Genotype[a]	Source[b] or reference
Escherichia coli K-12		
NU90	MC4100 Φ(*hisT'-lacZ*)*90*	M. Winkler (unpublished data)
NU399	NU426 *usg-1*::Km^r(*Pst*I)>	Arps et al. (2)
NU400	NU426 *pdxB*::Km^r(*Hin*dIII)>	2
NU402	NU426 *pdxB*::<Km^r(*Hin*dIII)	2
NU426	W3110 prototroph	Arps and Winkler (3)
NU543	CGSC 4805 *srl*::Tn*10 recA1*	CGSC 4805X P1 *kc* (TT9813)
NU544	CGSC 4805 *srl*::Tn*10 recA*$^+$	CGSC 4805X P1 *kc* (TT9813)
NU605	NU426 *pdxB*::<Km^r(*Bgl*I)	3
NU606	NU426 *pdxB*::Km^r(*Bgl*I)>	3
NU608	NU426 *pdxB*::<Km^r(*Eco*RV)	3
NU609	NU426 *pdxB*::Km^r(*Eco*RV)>	3
TT9813	TR6548 *srl*::Tn*10 recA1*	Hughes and Roth (29)
Other *E. coli* subspecies		
CGSC 2507 (*E. coli* B)	Wild type	B. Bachmann collection
CGSC 3121 (*E. coli* C)	Wild type	B. Bachmann collection
CGSC 4805 (*E. coli* B/K hybrid)	*pdxB5 hisG1 lac gal-6 rpsL tsx-65*	B. Bachmann collection
EB145 (*E. coli* B/r)	*dau-5 rpsL*	Searles et al. (42)
Klebsiella aerogenes	Wild type	B. Nichols collection
Salmonella typhimurium LT2		
Ames wild type	Wild type	P. Hartman collection
ara-9	*ara-9*	P. Hartman collection
Serratia marcescens	Wild type	B. Nichols collection
Plasmids		
pBR322	Replicon ColE1; Ap^r Tc^r	Bolivar et al. (10)
pBR325	Replicon ColE1; Ap^r Cm^r Tc^r	Prentki et al. (40)
pUC9	Replicon ColE1; *lacP* (polylinker) *lacZ*; Ap^r	Vieira and Messing (52)
pNU86	pBR322(*Hpa*I (640)-*Cla*I (3836)); Ap^r	3
pNU91	pNU86 [*pdxB*::Km^r(*Hin*dIII)>]; Ap^r Km^r	Km^r into *Hin*dIII (1518)
pNU92	pNU86 [*pdxB*::<Km^r(*Hin*dIII)]; Ap^r Km^r	Km^r into *Hin*dIII (1518)
pNU93	pBR322 (*Bgl*II (1)-*Cla*I (3836)); Ap^r	3
pNU97	pNU86 [*pdxB*::<Km^r(*Bgl*I)]; Ap^r Km^r	3
pNU102	pNU86 [*pdxB*::<Km^r(*Eco*RV)]; Ap^r Km^r	3
pNU117	pBR322 (*Hin*dIII (1518)-*Bgl*I (1784)); Ap^r; *pdxB* probe	Fragment ligated to pBR322 (*Hin*dIII-*Nru*I)
pNU118	pBR325 (*Eco*RI (2086)-*Eco*RI (2737)); Ap^r Tc^r; *usg-1* probe	Fragment ligated to pBR325 (*Eco*RI-*Eco*RI)
pNU119	pUC9 (*Taq*I (3133)-*Sau*3A (3636)); Ap^r; *hisT* probe	Fragment ligated to pUC9 (*Eco*RI-*Pst*I)

[a] < or > indicates that the direction of transcription of *kan* in the Km^r cassette is opposite to or the same as *hisT*, respectively. The restriction sites and the numbers used to designate them refer to the map in Fig. 1. For clarity, *usg-2* is referred to as *pdxB* as shown in this paper. Km^r (restriction site) signifies the presence of a kanamycin resistance cassette cloned into that site, whereas Km^r used as a phenotype indicates kanamycin resistance. Cm^r, Chloramphenicol resistant; Tc^r, tetracycline resistant; Ap, Ampicillin resistant.

[b] NU543 and NU544 were distinguished by UV sensitivity (37). In plasmid constructions, ends of fragments were made compatible by converting sites to blunt ends before ligation (2, 36).

the *hisT* operon, we constructed mutants containing Km^r cassette insertions near *hisT* in the bacterial chromosome (Fig. 1) (3). Insertions at the three closely spaced sites designated as *Eco*RV (1450), *Hin*dIII (1518), and *Bgl*I (1784) in Fig. 1 caused the same set of distinct phenotypes described below; therefore, we concluded that these three sites are within the same gene (*usg-2*) located upstream from *hisT* (2, 3). Furthermore, evidence presented in the accompanying paper demonstrates conclusively that *usg-2* and *hisT* are members of the same operon (3) (Fig. 1). Growth of the *usg-2*::Km^r mutants was indistinguishable from that of the prototrophic parent strain on LB + Cys medium at 25, 30, 37, and 42°C (data not shown). By contrast, *usg-2*::Km^r mutants did not readily grow on minimal (E) plus glucose medium at 37 and 42°C (Table 2, lines 2 and 3). However, the *usg-2*::Km^r mutants did form oddly translucent, mucoid colonies on minimal medium at 25 and 30°C (Table 2, line 1; Fig. 2, upper panels). As noted in Table 2, the phenotypes of *usg-2* mutants were the same for Km^r cassette insertions in either possible orientation at the three sites marked in Fig. 1. In addition, it should be recalled that Km^r cassettes are not transposons and cause stable disruptions of genes (3, 54). Thus, these insertion mutations were unusual because they resulted in conditional auxotrophy.

When we examined bacterial cells by light and electron microscopy, we were surprised to find that the *usg-2*::Km^r mutants formed spherical cells on minimal (E) plus glucose medium at 25 and 30°C (Fig. 2, lower panels). Control experiments with *usg-1*::Km^r and *hisT*::Km^r mutants established that the presence of the Km^r cassette per se in this region of the chromosome was not responsible for the spherical cell shape. These spherical cells had another

TABLE 2. Colony and cellular morphologies of *usg-2*::Km^r mutants[a]

Growth medium[b]	Temp (°C)	Morphology[c]	
		NU426 (W3110 parent)	NU402 (*usg-2*::Km^r)
Minimal (E) + glucose	≤30	Med; opaque (rods)	Sm; translucent, mucoid (mainly round; some irregular)
	37	Med; opaque (rods)	NG
	42	Med; opaque	NG
Minimal (E) + glucose + D-Ala	≤30	Med; opaque (rods)	Sm; partially translucent, mucoid (rods)
	37	Med; opaque (rods)	Sm; opaque (rods)
	42	Med; opaque	Very sm; opaque
Minimal (E) + glucose + ACH + L-Trp	≤30	Lg; opaque	NG
	37	Lg; opaque	NG
	42	Lg; opaque	NG

[a] The first part of each entry describes relative colony size and appearance, and the second part in parentheses gives the cell shape viewed in the light or electron microscope.

[b] Bacteria were streaked from patches on an LB + Cys (NU426) or LB + Cys + kanamycin (NU402) plate onto prewarmed plates, which were incubated for 24 to 48 h at the temperatures indicated. Supplements were added at the following final concentrations: glucose, 0.4% (wt/vol); D-alanine, 1 mM; ACH (vitamin assay Casamino Acids), 0.5% (wt/vol); L-tryphophan, 0.1 mM.

[c] Other *usg-2*::Km^r mutants (NU400, NU605, NU606, NU608, NU609) gave the same results as NU402. Strains NU400(pNU93) and NU400(pNU86), whose recombinant plasmids contain the *Bgl*II (1)-*Cla*I (3836) and the *Hpa*I (640)-*Cla*I (3836) fragments, respectively (Fig. 1; Table 1), had the same phenotype as the parent strain NU426. By contrast, the characteristics of strains NU400(pNU91) and NU400(pNU92), which contain *usg-2*::Km^r(*Hin*dIII)> and *usg-2*::<Km^r(*Hin*dIII) mutations in plasmid pNU86, respectively, matched those of NU402. Lg, Large; Med, medium; Sm, small; NG, no growth.

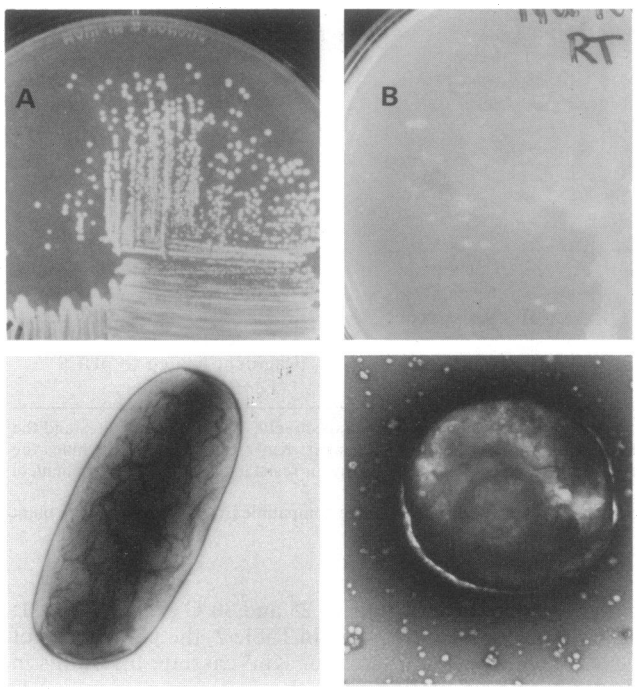

FIG. 2. Colony morphology and cell structure of *usg-2*::Km^r mutants. Bacteria were streaked onto plates containing minimal (E) plus glucose medium which were incubated for 2 to 3 days at room temperature (~25°C). Similar results were obtained when plates were incubated at 30°C (Table 2). Plates were photographed with a Polaroid MP4 camera, and portions of colonies were prepared for electron microscopy as described in the Materials and Methods. Upper photos show the appearance of bacterial colonies, and lower photos show typical cells from one of the colonies. The magnification of the electron micrographs is ×19,990. (A) Prototrophic parent strain, NU426. (B) *usg-2*::Km^r(*Hin*dIII)> mutant, NU400. Similar results were obtained for the other *usg-2*::Km^r mutants listed in Table 2.

unusual property in that they appeared to divide evenly along their equators (21). We reasoned that the round shape might be caused by an inability of the cells to synthesize peptidoglycan efficiently; hence, the cells are forced to assume the shape of the geometrically simple sphere with its lower ratio of surface area to volume than the more complicated rod. We tested this notion by adding D-alanine, which is a primary component of the bacterial cell wall, to the minimal (E) plus glucose medium. Addition of D-alanine restored the shape of *usg-2*::Km^r mutants to rods and partially prevented temperature sensitivity (Table 2). However, D-alanine did not completely eliminate the translucent, mucoid appearance of the *usg-2*::Km^r colonies at 30°C, even though the cells were rod shaped (Table 2, line 1).

Several other properties of the *usg2*::Km^r mutants are noteworthy. When these mutants were streaked onto minimal (E) plus glucose plates containing all 20 common amino acids, they failed to grow even at 30°C (Table 2, last section). In addition, when *usg-2*::Km^r mutants were left on minimal (E) plus glucose plates at 37 or 42°C for 3 or more days, relatively fast-growing pseudorevertants appeared (data not shown). These pseudorevertants had to contain compensatory second-site mutations that allowed growth on minimal (E) plus glucose medium at higher temperatures because they retained their resistance to kanamycin. Furthermore, the different pseudorevertant isolates showed a range of heritable phenotypes including formation of relatively fast-growing translucent colonies and formation of relatively slow-growing opaque colonies. As described in the Discussion, the array of phenotypes shown by *usg-2*::Km^r mutants can be readily understood in terms of the pyridoxine biosynthetic pathway.

***usg-2* is *pdxB*.** The observation that *usg2*::Km^r insertions caused temperature-sensitive auxotrophy and could be suppressed by second-site mutations was initially confusing and did not seem to match phenotypes expected for mutations that had previously been mapped near 50 min in the bacterial chromosome (4). However, as we characterized the *usg-2*::Km^r mutants further, we found that some of the phenotypes were the same as those noted by Dempsey and his

TABLE 3. Compounds that support growth of *usg-2*::Km^r mutants at 37 and 42°C[a]

Strain[b]	Temp (°C)	Growth on[c]: None	POX	PAL	PAM	GLYC	PYR	D-Ala
NU402 [*usg-2*::<Km^r(*Hin*dIII)]	37	−	++	++	++	+	+/−	+
	42	−	++	++	++	+/−	+/−	+/−
NU400 [*usg-2*::Km^r(*Hin*dIII)>]	37	−	++	++	++	+	+/−	+
	42	−	++	++	++	+/−	+/−	+/−

[a] Bacteria were grown in LB + Cys medium at 37°C, collected by centrifugation, washed several times with minimal (E) plus 0.4% glucose medium, and spread onto prewarmed plates containing minimal (E) plus 0.4% glucose medium. Crystals of compounds were placed on the plates, which were incubated for about 18 h at 37 or 42°C and scored for zones of growth.

[b] The same results were obtained for strains NU605 and NU608, which contain *usg-2*::<Km^r(*Bgl*I) and *usg-2*::<Km^r(*Eco*RV) insertion mutations, respectively (Fig. 1).

[c] POX, Pyridoxine hydrochloride; PAL, pyridoxal hydrochloride; PAM, pyridoxamine dihydrochloride (>98%); GLYC, glycolaldehyde; PYR, 4-pyridoxic acid; D-Ala, D-alanine. About 50 other vitamins, amino acids, cofactors, metabolic intermediates, purine bases, and pyrimidine bases did not support growth of these strains (see text). −, No growth; ++, heavy growth; +, good growth; +/−, marginal growth.

associates when they defined and localized the *pdxB* locus (16–18, 20, 46). In particular, pyridoxine, pyridoxal, pyridoxamine, and glycolaldehyde supported growth of *usg-2*::Km^r mutants at 37°C (Table 3). Even 4-pyridoxic acid, which is a catabolic derivative of pyridoxal, caused a limited growth response, perhaps by backward seepage of the catabolic pathway. It should be noted that our samples of 4-pyridoxic acid and pyridoxamine, which appears not to be taken up by *E. coli* or *Salmonella typhimurium* (15, 39), were not purified or analyzed by us; consequently, they may be slightly contaminated with pyridoxine or pyridoxal. As expected from the results presented in the last section, D-alanine also enabled growth of the mutants, especially at 37°C (Table 3). The other two unusual amino acids that form the peptidoglycan of *E. coli*, D-glutamine and *meso*-diaminopimelic acid, as well as about 50 other compounds failed to support growth of *usg-2*::Km^r mutants in our spot tests (Table 3, footnote *c*).

To prove that *usg-2* corresponds to the *pdxB* locus of Dempsey (18), we completed the *trans* test shown in Table 4. Plasmids pNU86 and pNU93, which contain the *Hpa*I (640)-*Cla*I (3836) and *Bgl*II (1)-*Cla*I (3836) fragments, respectively (Fig. 1; Table 1), complemented the original *pdxB5* mutation of Dempsey (Table 4; data not shown) and restored our *usg-2*::Km^r mutants to the phenotypes of the W3110 parent strain (Table 2, footnote *c*). In contrast, derivatives of pNU86 containing Km^r cassettes at *Eco*RV (1450), *Hin*dIII (1518), or *Bgl*I (1784) interfered with the complementation of the *pdxB5* allele (Table 4, top part). We assumed that the single colonies that appeared in our *trans* test arose from recombination between the bacterial chromosome and the plasmids. To test this idea and obtain a cleaner result, we repeated the complementation experiment in a *pdxB5 recA1* mutant. The plasmids containing the Km^r cassettes failed to complement *pdxB5* in the *recA1* background (Table 4). We can interpret this *trans* test by taking into account the following additional information. (i) The direction of transcription of *usg-2* on the recombinant plasmids is known (Fig. 1) (2, 3); (ii) genes downstream from *usg-2* on the recombinant plasmids do not seem to be involved in vitamin B_6 metabolism (see above) (2, 3); (iii) plasmid pNU86, which complemented *pdxB5* (Table 4), contains just enough chromosomal insert DNA to account for the size of the *usg-2* gene product (Fig. 1) (3); and (iv) *recA*$^+$-dependent recombination that resulted in a Pdx$^+$ phenotype seemed to occur in the *usg-2* region between derivatives of pNU86 and the chromosome of the *pdxB5* mutant (Table 4). Taken together, these observations allow us to conclude that *usg-2* is the same as the *pdxB* locus of Dempsey.

Evolutionary conservation of the association of *pdxB*, *usg-1*, and *hisT*. We wanted to learn whether *pdxB*, *usg-1*, and *hisT* are closely associated in *E. coli* subspecies other than K-12 and in enterobacterial species other than *E. coli*. Consequently, we performed Southern hybridization experiments

TABLE 4. Complementation pattern of *pdxB5* by plasmids containing wild-type or mutant *usg-2*

Background strain[a]	Relevant genotype of background strain	Plasmid[b]	Genotype of *usg-2* on plasmid	Growth on minimal (E) + glucose + L-His + ampicillin medium[c]
NU544	*hisG1 pdxB5*	pNU86	*usg-2*$^+$	+
		pNU91	*usg-2*::Km^r(*Hin*dIII)>	Single colonies
		pNU92	*usg-2*::<Km^r(*Hin*dIII)	Single colonies
		pNU97	*usg-2*::<Km^r(*Bgl*I)	Single colonies
		pNU102	*usg-2*::<Km^r(*Eco*RV)	Single colonies
NU543	*hisG1 pdxB5 recA1*	pNU86	*usg-2*$^+$	+
		pNU91	*usg-2*::Km^r(*Hin*dIII)>	−
		pNU92	*usg-2*::<Km^r(*Hin*dIII)	−
		pNU97	*usg-2*::<Km^r(*Bgl*I)	−
		pNU102	*usg-2*::<Km^r(*Eco*RV)	−

[a] Background strains were derived from CGSC 4805 (Table 1). The *pdxB5* allele was originally isolated by Dempsey, who used it to locate *pdxB* (18).

[b] Plasmid pNU86 contains the ~3,200-bp *Hpa*I (640)-*Cla*I (3836) fragment cloned into pBR322 (Table 1; Fig. 1). The other plasmids are derivatives of pNU86 containing Km^r cassettes at the sites and in the orientations indicated.

[c] Single colonies of each strain were streaked onto plates, which were incubated at 37°C for about 48 h. Supplements were added at the following final concentrations: glucose, 0.4%; L-histidine, 0.1 mM; ampicillin, 50 μg/ml. +, Heavy, contiguous growth and formation of single colonies; single colonies, no heavy, contiguous growth but formation of between 20 and 200 single colonies per plate; −, no growth.

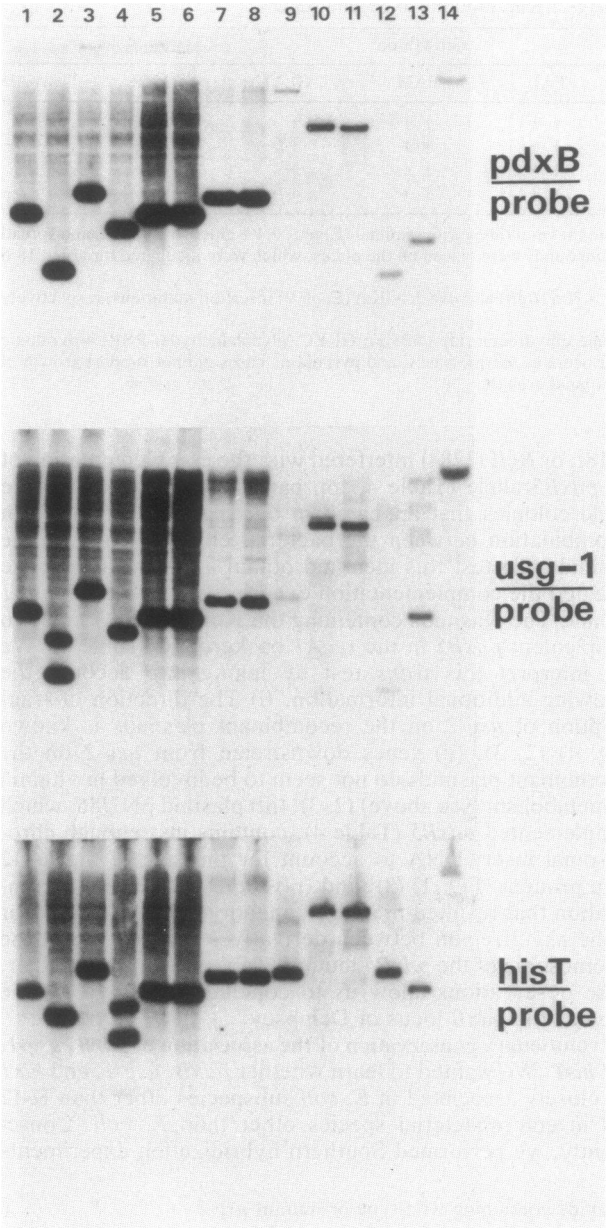

FIG. 3. Moderately high stringency Southern hybridizations between probes from genes in the *E. coli* K-12 *hisT* operon and genomic DNA from different enterobacterial species. Isolation of genomic DNA, preparation of probes from the coding regions of *pdxB*, *usg-1*, and *hisT*, and hybridization conditions are detailed in the Materials and Methods. The lanes contain genomic DNA isolated from the following strains (Table 1): 1, NU426 (*E. coli* K-12); 2, NU399; 3, NU400; 4, NU90; 5, CGSC 2507 (*E. coli* B); 6, CGSC 3121 (*E. coli* C); 7, Ames wild type (*S. typhimurium* LT2); 8, *ara-9* (*S. typhimurium* LT2); 9 to 11, *K. aerogenes* wild type; 12 and 13, *S. marcescens* wild type; 14, phage λ standard. Genomic DNA samples were digested with the following restriction endonucleases before resolution on agarose gels: lanes 1 to 6 and 9, *Hin*dIII plus *Cla*I; lanes 7, 8, and 11, *Sal*I; lanes 10 and 12, *Pst*I; lane 13, *Eco*RI; lane 14, *Hin*dIII.

like the ones depicted in Fig. 3. The three probes for the coding regions of *pdxB*, *usg-1*, and *hisT* were the *Hin*dIII (1518)-*Bgl*I (1784), *Eco*RI (2086)-*Eco*RI (2737), and *Taq*I (3133)-*Sau*3A (3636) restriction fragments, respectively (Fig. 1; Table 1). Lanes 1 to 4 show control experiments. As expected (Fig. 1), all three probes hybridized to the same 2,300-base pair (bp) fragment from a *Hin*dIII plus *Cla*I digestion of W3110 *E. coli* K-12 genomic DNA (lane 1). Lanes 2 to 4 show the hybridization patterns predicted for *Hin*dIII plus *Cla*I digestions of genomic DNA isolated from *E. coli* K-12 *usg-1*::Km^r(*Pst*I (2579)) (lane 2), *pdxB*::Km^r(*Hin*dIII (1518)) (lane 3), and Φ(*hisT'-lacZ*) (lane 4) mutants. The significant point from these three controls is that they confirm the specificity of the probes. For example, in lane 2 the *usg-1* probe hybridized to two fragments, whereas the *pdxB* or *hisT* probes hybridized to only the smaller or larger of the two fragments, respectively.

Other lanes in Fig. 3 indicate that *pdxB*, *usg-1*, and *hisT* are contained on the same 2,300-bp fragment in *E. coli* B (lane 5) and *E. coli* C (lane 6), on the same 2,800-bp fragment in *S. typhimurium* (lanes 7 and 8), and on the same 6,600-bp fragment in *Klebsiella aerogenes* (lanes 10 and 11). Lanes 9 and 13 show that *usg-1* and *hisT* are located on the same 2,900- or 2,300-bp fragment of *K. aerogenes* or *Serratia marcescens*, respectively, but do not allow any conclusions to be made about the proximity of *pdxB*. However, experiments not shown in Fig. 3 strongly suggest that *pdxB* is closely associated with *usg-1* and *hisT* in *S. marcescens* and possibly in *Proteus mirabilis* as well. Other unpublished experiments demonstrate that *E. coli* B/r seems to have the same restriction map in the region around the *hisT* operon as the *E. coli* subspecies in Fig. 3. This result suggests that the inability to map *hisT* (*leuK*) mutations of *E. coli* B/r near *purF* in interspecies crosses (42) probably was caused by technical difficulties rather than a radical difference in the structure or location of the *E. coli* B/r *hisT* operon. Finally, we performed experiments analogous to those in Fig. 3 using low stringency hybridization conditions (see Materials and Methods). With each of the three probes, we failed to detect additional bands that would imply significant conservation of sequences among members of the *pdx* regulon (17, 18, 20, 43) or pseudouridine synthase gene family (44). In conclusion, these combined results show that *pdxB*, *usg-1*, and *hisT* contain unique nucleotide sequences in *E. coli* K-12 and that these three genes are closely associated in several enterobacterial species. This close association is consistent with the notion that *pdxB*, *usg-1*, and *hisT* form a complex operon in enterobacteria other than *E. coli* K-12.

DISCUSSION

In this paper, we establish genetically that *usg-2*, which is upstream of *hisT* in the same operon, is actually *pdxB*, which mediates the biosynthesis of the B_6 vitamer pyridoxine (Table 4). This finding suggested that we might understand the diverse phenotypes of our *pdxB*::Km^r cassette mutants by considering the pyridoxine and pyridoxal phosphate biosynthetic pathways. Consequently, we reviewed the isotope-labeling experiments of Spenser and his associates (25, 50, 51) and the physiological and biochemical experiments of Dempsey and his associates (16, 46, 53) and compiled the summary shown in Fig. 4. The *pdxB* gene mediates the placement of carbons 5, 5', and 6 into the pyridine ring of pyridoxine. It should be noted that formation of the pyridine ring of pyridoxine and pyridoxal phosphate occurs by an entirely different route from the one used to synthesize the pyridine ring of NAD (28). Carbons 5, 5', and 6 can also be added to the ring by an extremely low-level alternative pathway that uses the two-carbon compound glycolaldehyde as an intermediate (46, 50) (Fig. 4).

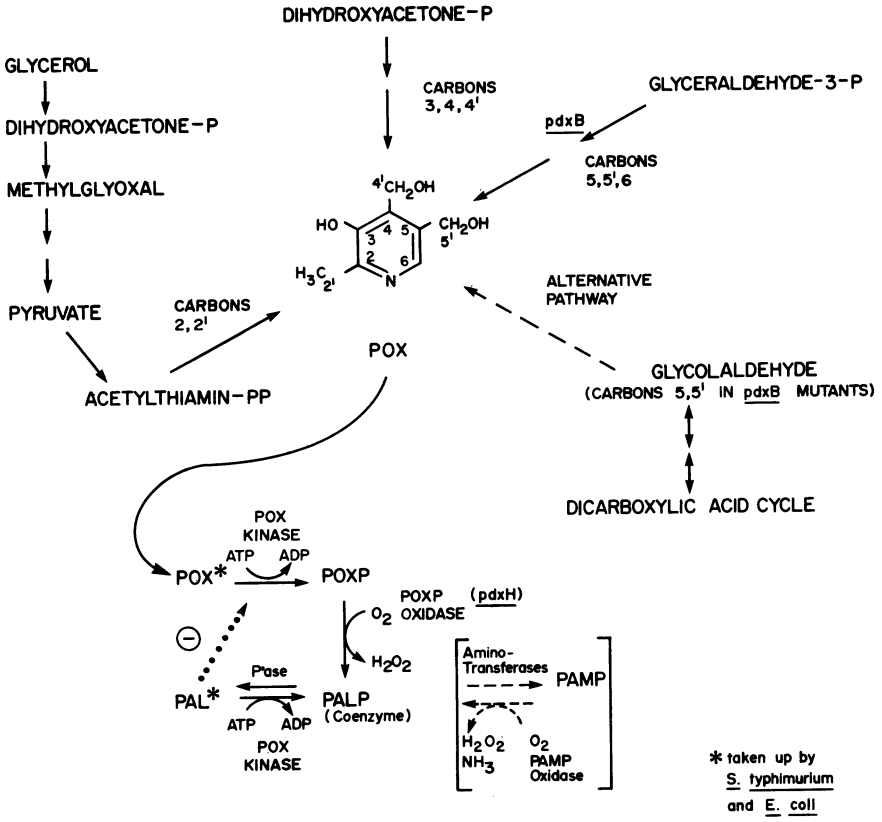

FIG. 4. Biosynthetic pathway of pyridoxine and pyridoxal phosphate in *E. coli* K-12. This scheme was compiled from the work of Dempsey, Spenser, and their associates (see text). It is assumed that endogenous glycolaldehyde is synthesized by pathways related to the dicarboxylic acid cycle. The dotted arrow from pyridoxal to pyridoxine kinase indicates that pyridoxal is a negative effector of kinase activity (53). Of the dispersed genes that form the *pdx* regulon, only the function of *pdxH*, which encodes pyridoxine phosphate oxidase, is known (43). Abbreviations: POX, pyridoxine; POXP, pyridoxine phosphate; PALP, pyridoxal phosphate; PAL, pyridoxal; PAMP, pyridoxamine phosphate.

We suggest that our *pdxB*::Km^r cassette mutants grow on minimal (E) plus glucose medium at 25 and 30°C (Fig. 2; Table 2) because a limited amount of pyridoxine is synthesized by the alternative pathway. This in turn limits the amount of D-alanine available for peptidoglycan biosynthesis, because L-alanine:D-alanine racemase is a pyridoxal phosphate-dependent enzyme. Lack of D-alanine seems to be a primary cause of the spherical shape assumed by *pdxB*::Km^r cells on minimal (E) plus glucose medium at 30°C and below (Tables 2 and 3). In addition, we suggest that the *pdxB*::Km^r mutants fail to grow at 37 and 42°C without supplementation, because they are unable to synthesize sufficient peptidoglycan to form stable cell walls. This interpretation is supported by the observation that the *pdxB*::Km^r mutants did grow slowly at high temperatures on minimal (E) plus glucose medium containing D-alanine (Tables 2 and 3). This line of reasoning is also entirely consistent with compounds other than D-alanine that supported growth of the *pdxB*::Km^r mutants at 37 and 42°C (Table 3). In particular, growth of *pdxB* mutants would be expected in the presence of pyridoxine, pyridoxal, and glycolaldehyde based on the pathway shown in Fig. 4.

Furthermore, we can gain insight into the types of second-site mutations that would lead to the appearance of temperature-resistant, kanamycin-resistant *pdxB*::Km^r pseudorevertants (see Results). These pseudorevertants fell into several phenotypic classes which argues that there are probably several ways to compensate for a *pdxB*::Km^r knockout mutation. We suggest that second-site mutations that increase the efficiency of the alternative pathway, that increase the ability of the cell to synthesize peptidoglycan during pyridoxal phosphate limitation, and that cause loss of control of pyridoxine biosynthesis or intermediary metabolism might be found among the *pdxB*::Km^r pseudorevertants. By considering the scheme for pyridoxine biosynthesis (Fig. 4), we can also speculate why amino acid addition inhibited the growth of *pdxB*::Km^r mutants on minimal (E) plus glucose medium at 30°C (Table 2). Preliminary studies suggest that cells adjust their rate of pyridoxal phosphate biosynthesis by sensing the levels of certain amino acids such as threonine (19). Therefore, addition of amino acids might repress branches of the pyridoxine biosynthetic pathway to such an extent that the alternative pathway is unable to synthesize even limiting amounts of pyridoxine. This hypothesis and the identity of the *pdxB*::Km^r pseudorevertants need to be further analyzed genetically.

We also show in this paper that the close association of *pdxB* and *hisT* is evolutionarily conserved in several enterobacterial species (Fig. 3). This finding is consistent with the notion that *pdxB* and *hisT* are members of a complex operon in enterobacterial species other than *E. coli* K-12. As noted in the Introduction, the reasons genes are grouped into multifunctional operons are not generally well understood. For the macromolecular synthesis (sigma) operon, it is

assumed that *rpsU*, *dnaG*, and *rpoD* are arranged together because they are involved in the initiation steps of translation, DNA replication, and RNA transcription (34). For the *serC-aroA* operon, it can convincingly be argued that coordinate expression of the prechorismate and serine biosynthetic pathways is required to guarantee efficient synthesis of enterochelin when bacteria are starved for iron (23, 26). At this point in our study, we can only speculate about why *pdxB* and *hisT* are in the same operon. The endpoint of the pathway mediated by *pdxB* is pyridoxal phosphate. This vital coenzyme is involved in the metabolism of nearly every amino acid (6). Therefore, pyridoxal phosphate availability might act to modulate enzyme activities and contribute to the flow of intermediates down certain amino acid metabolic pathways. On the other hand, it has been suggested that stress conditions such as amino acid starvation result in undermodifications in the anticodon stem and loop of specific tRNA species (11, 32, 48). These undermodified tRNA molecules could then cause defects in attenuation control and thereby increase the expression of certain genes and operons (11, 24, 48). Although definitive results are lacking, it has long been suspected that the pseudouridine residues synthesized by the *hisT* gene product play such a regulatory role in modulating attenuation control of amino acid biosynthetic operons (32, 48). Thus, through entirely different mechanisms, both *pdxB* and *hisT* potentially can act as control loci in the global regulation of amino acid metabolism. The arrangement of these two control loci into the same operon could allow coordinate expression in response to certain metabolic conditions.

Three additional observations are relevant to considerations about why *pdxB* and *hisT* are in the same operon. First, it is intriguing that *pdxA*, which encodes another pyridoxine biosynthetic gene located at a different position from *pdxB* in the bacterial chromosome, and *ksgA*, which encodes an rRNA modification enzyme, may also form a complex operon in *E. coli* K-12 (1, 49). If this inference is correct, it could suggest that the presence of coenzyme biosynthetic genes in multifunctional operons is a way to interweave the regulation of coenzyme biosynthesis into general cellular metabolism. More information about the biosynthesis of cofactors such as pyridoxal phosphate is required to test this hypothesis. Second, Björk and his associates (8, 12) have shown that at least one other tRNA modification gene, *trmD*, is a member of a multifunctional operon. Presently, only a small fraction of the 50 or more genes that encode bacterial RNA modification enzymes has been analyzed in detail (8). Therefore, the arrangement of tRNA modification genes into complex operons might be a rather general feature in enterobacteria. Finally, several previous studies have established unusual links between tRNA modification and intermediary metabolism (7, 8, 11, 24, 31). The results presented here add to these observations and emphasize the need to learn more about the functions of modifications in stable RNA molecules.

ACKNOWLEDGMENTS

We thank B. Bachmann, J. Calvo, P. Hartman, K. Hughes, B. Nichols, B. Tyler, and J. Roth for strains, R. Dhaliwal for help with Southern blotting, S. Hultgren for help with electron microscopy, R. Rownd and D. Womble for access to equipment, and M. Johnson and L. Taylor for help with preparation of the manuscript. We also thank M. Connolly, B. Nichols, R. Scarpulla, and G. Walker for protocols and stimulating discussions.

This work was supported by grant DMB-8417005 from the National Science Foundation.

LITERATURE CITED

1. **Andresson, O. S., and J. E. Davies.** 1980. Genetic organization and restriction enzyme cleavage map of the *ksgA-pdxA* region of the *Escherichia coli* chromosome. Mol. Gen. Genet. **179**:211–216.
2. **Arps, P. J., C. C. Marvel, B. C. Rubin, D. R. Tolan, E. E. Penhoet, and M. E. Winkler.** 1985. Structural features of the *hisT* operon of *Escherichia coli* K-12. Nucleic Acids Res. **13**:5297–5315.
3. **Arps, P. J., and M. E. Winkler.** 1986. Structural analysis of the *Escherichia coli* K-12 *hisT* operon by using a kanamycin resistance cassette. J. Bacteriol. **169**:1061–1070.
4. **Bachmann, B. B.** 1983. Linkage map of *Escherichia coli* K-12, edition 7. Microbiol. Rev. **47**:180–230.
5. **Beckwith, J., J. Davies, and J. A. Gallant (ed.).** 1983. Gene function in prokaryotes. Cold Spring Harbor Laboratory, Cold Spring Harbor, N.Y.
6. **Bender, D. A.** 1985. Amino acid metabolism. John Wiley & Sons, Inc., New York.
7. **Björk, G. R.** 1980. A novel link between the biosynthesis of aromatic amino acids and transfer RNA modification in *Escherichia coli*. J. Mol. Biol. **140**:391–410.
8. **Björk, G. R.** 1984. Modified nucleosides in RNA—their formation and function, p. 292–330. *In* D. Apirion (ed.), Processing of RNA. CRC Press, Inc., Boca Raton, Fla.
9. **Björk, G. R.** 1985. *E. coli* ribosomal protein operons: the case of the misplaced genes. Cell **42**:7–8.
10. **Bolivar, F., R. L. Rodriguez, P. J. Greene, M. C. Betlach, H. L. Heynecker, H. W. Boyer, J. H. Crosa, and S. Falkow.** 1977. Construction and characterization of new cloning vehicles. II. A multipurpose cloning system. Gene **2**:95–113.
11. **Buck, M., and B. N. Ames.** 1984. A modified nucleotide in tRNA as a possible regulator of aerobiosis: synthesis of *cis*-2-methylthioribosylzeatin in the tRNA of *Salmonella*. Cell **36**:523–531.
12. **Byström, A. S., K. J. Hjalmarsson, P. M. Wikström, and G. R. Björk.** 1983. The nucleotide sequence of an *Escherichia coli* operon containing genes for the tRNA (m'G) methyltransferase, the ribosomal proteins S-16 and L-19, and a 21 kilodalton polypeptide. EMBO J. **2**:899–906.
13. **Dabbs, J.** 1984. Order of ribosomal protein genes in the *rif* cluster of *Bacillus subtilis* is identical to that of *Escherichia coli*. J. Bacteriol. **159**:770–772.
14. **Davis, R. W., D. Botstein, and J. R. Roth.** 1980. Advanced bacterial genetics. Cold Spring Harbor Laboratory, Cold Spring Harbor, N.Y.
15. **Dempsey, W. B.** 1965. Control of pyridoxine biosynthesis in *Escherichia coli*. J. Bacteriol. **90**:431–437.
16. **Dempsey, W. B.** 1966. Synthesis of pyridoxine by a pyridoxal auxotroph of *Escherichia coli*. J. Bacteriol. **92**:333–337.
17. **Dempsey, W. B.** 1969. Characterization of pyridoxine auxotrophs of *Escherichia coli*: P1 transduction. J. Bacteriol. **97**:1403–1410.
18. **Dempsey, W. B.** 1969. Characterization of pyridoxine auxotrophs of *Escherichia coli*: chromosomal position of linkage group I. J. Bacteriol. **100**:295–300.
19. **Dempsey, W. B.** 1982. Threonine prevents derepression of pyridoxine synthesis in *Escherichia coli* B. J. Bacteriol. **150**:1476–1478.
20. **Dempsey, W. B., and P. F. Pachler.** 1966. Isolation and characterization of pyridoxine auxotrophs of *Escherichia coli*. J. Bacteriol. **91**:642–645.
21. **Donachie, W. D., K. J. Begg, and N. F. Sullivan.** 1984. Morphogenes of *Escherichia coli*, p. 27–62. *In* R. Losick and L. Shapiro (ed.), Microbial development. Cold Spring Harbor Laboratory, Cold Spring Harbor, N.Y.
22. **Driver, R. P., and R. P. Lawther.** 1985. Physical analysis of deletion mutations in the *ilvGEDA* operon of *Escherichia coli* K-12. J. Bacteriol. **162**:598–606.
23. **Duncan, K., and J. R. Coggins.** 1986. The *serC-aroA* operon of *Escherichia coli*. A mixed function operon encoding enzymes from two different amino acid biosynthetic pathways. Biochem. J. **214**:49–57.
24. **Ericson, J. U., and G. R. Björk.** 1986. Pleiotropic effects

induced by modification deficiency next to the anticodon of tRNA from *Salmonella typhimurium* LT2. J. Bacteriol. **166**:1013–1021.
25. **Hill, R. E., F. J. Rowell, R. N. Gupta, and I. D. Spenser.** 1972. Biosynthesis of vitamin B6. J. Biol. Chem. **247**:1869–1882.
26. **Hoiseth, S. K., and B. A. D. Stocker.** 1985. Genes *aroA* and *serC* of *Salmonella typhimurium* constitute an operon. J. Bacteriol. **163**:355–361.
27. **Hoopes, B. C., and W. R. McClure.** 1981. Studies on the selectivity of DNA precipitation of spermine. Nucleic Acids Res. **9**:5493–5504.
28. **Hughes, K. T., B. T. Cookson, D. Ladika, B. M. Olivera, and J. R. Roth.** 1983. 6-Aminonicotinamide-resistant mutants of *Salmonella typhimurium*. J. Bacteriol. **154**:1126–1136.
29. **Hughes, K. T., and J. R. Roth.** 1984. Conditionally transposition-defective derivative of Mu dl (Ap *lac*). J. Bacteriol. **159**:130–137.
30. **Hultgren, S. J., T. N. Proter, A. J. Schaeffer, and J. L. Duncan.** 1985. Role of type 1 pili and effects of phase variation on lower urinary tract infections produced by *Escherichia coli*. Infect. Immun. **50**:370–377.
31. **Kersten, H.** 1984. On the biological significance of modified nucleosides in tRNA. Prog. Nucleic Acid Res. Mol. Biol. **31**:59–113.
32. **Kitchigman, G. R., and M. J. Fournier.** 1977. Modification deficient ribonucleic acids from relaxed control *Escherichia coli*: structure of the major undermodified phenylalanine and leucine transfer RNAs produced during leucine starvation. Biochemistry **16**:2213–2220.
33. **Lewin, B.** 1985. Genes II. John Wiley & Sons, Inc., New York.
34. **Lupski, J. R., and G. N. Godson.** 1984. The *rpsU-dnaG-rpoD* macromolecular synthesis operon of *E. coli*. Cell **39**:251–252.
35. **Maniatis, T., E. F. Fritsch, and J. Sambrook.** 1982. Molecular cloning, a laboratory manual. Cold Spring Harbor Laboratory, Cold Spring Harbor, N.Y.
36. **Marvel, C. C., P. J. Arps, B. C. Rubin, H. O. Kammen, E. E. Penhoet, and M. E. Winkler.** 1985. *hisT* is part of a multigene operon in *Escherichia coli* K-12. J. Bacteriol. **161**:60–71.
37. **Miller, J. H.** 1972. Experiments in molecular genetics. Cold Spring Harbor Laboratory, Cold Spring Harbor, N.Y.
38. **Miller, J. H., and W. S. Reznikoff (ed.).** 1978. The operon. Cold Spring Harbor Laboratory, Cold Spring Harbor, N.Y.
39. **Mulligan, J. H., and E. E. Snell.** 1976. Transport and metabolism of vitamin B6 in *Salmonella typhimurium* LT2. J. Biol. Chem. **251**:1052–1056.
40. **Prentki, P., F. Karch, S. Iida, and J. Meyer.** 1981. The plasmid cloning vector pBR325 contains a 482 base-pair-long inverted duplication. Gene **14**:289–299.
41. **Schleif, R.** 1986. Genetics and molecular biology. Addison-Wesley Publishing Co., Reading, Mass.
42. **Searles, L. L., J. W. Jones, M. J. Fournier, N. Grambow, B. Tyler, and J. M. Calvo.** 1986. *Escherichia coli* B/r *leuK* mutant lacking pseudouridine synthase I activity. J. Bacteriol. **166**:341–345.
43. **Shimizu, S., and W. B. Dempsey.** 1976. Genetic map position of the *pdxH* gene in *Escherichia coli*. J. Bacteriol. **127**:1593–1594.
44. **Singer, C. E., G. R. Smith, R. Cortese, and B. N. Ames.** 1972. Mutant $tRNA^{His}$ ineffective in repression and lacking two pseudouridine modifications. Nature (London) New Biol. **238**:72–74.
45. **Southern, E.** 1975. Detection of specific sequences among DNA fragments separated by gel electrophoresis. J. Mol. Biol. **98**:503–517.
46. **Tani, Y., and W. B. Dempsey.** 1973. Glycolaldehyde is a precursor of pyridoxal phosphate in *Escherichia coli* B. J. Bacteriol. **116**:341–345.
47. **Tillawella, I. P. B.** 1984. Evidence for clustering of RNA polymerase and ribosomal protein genes in six species of enterobacteria. Mol. Gen. Genet. **195**:215–218.
48. **Turnbough, C. L., R. J. Neill, R. Landsberg, and B. N. Ames.** 1979. Pseudouridylation of tRNAs and its role in regulation in *Salmonella typhimurium*. J. Biol. Chem. **254**:5111–5119.
49. **Van Buul, C. P. J. J., and P. H. van Knippenberg.** 1985. Nucleotide sequence of the *ksgA* gene of *Escherichia coli*: comparison of methyltransferases affecting dimethylation of adenosine in ribosomal RNA. Gene **38**:65–72.
50. **Vella, G. J., R. E. Hill, B. S. Mootoo, and I. D. Spenser.** 1980. The status of glycolaldehyde in the biosynthesis of vitamin B6. J. Biol. Chem. **255**:3042–3048.
51. **Vella, G. J., R. E. Hill, and I. D. Spenser.** 1981. Biosynthesis of pyridoxol. J. Biol. Chem. **256**:10469–10474.
52. **Vieira, J., and J. Messing.** 1982. The pUC plasmids, an M13 mp7-derived system for insertion mutagenesis and sequencing with synthetic universal primers. Gene **19**:259–268.
53. **White, R. S., and W. B. Dempsey.** 1970. Purification and properties of vitamin B6 kinase from *Escherichia coli* B. Biochemistry **9**:4057–4064.
54. **Winans, S. C., S. J. Elledge, J. H. Krueger, and G. C. Walker.** 1985. Site-directed insertion and deletion mutagenesis with cloned fragments in *Escherichia coli*. J. Bacteriol. **161**: 1219–1221.